

Antibodies Mimic Natural Oxidosqualene–Cyclase Action in Steroid Ring A Formation

Jens Hasserodt,* Kim D. Janda,* and Richard A. Lerner*

Contribution from the Department of Chemistry and The Skaggs Institute for Chemical Biology, The Scripps Research Institute, 10550 North Torrey Pines Road, La Jolla, California 92037

Received August 23, 1999

Abstract: Cationic cyclizations are among the most demanding reactions that have been catalyzed by antibodies. These studies provided valuable mechanistic insights while opening up the possibility of formation of steroidal carbon frameworks. However, they have involved substrates that contained an aryl sulfonate group adjacent to a primary carbon center not observed in natural cationic cyclization processes. This paper presents an extension of our earlier work, now focusing on substrates analogous to those seen in triterpene biosynthesis. Three antibodies, 15D6, 20C7, and 25A10, have been generated by immunization with an 4-aza-steroid aminoxide hapten (termed HA8) that initiate the cationic cyclization of an oxidosqualene derivative and catalyze the formation of ring A of the lanosterol nucleus at neutral pH. Antibody HA8-25A10 kinetically resolved its racemic substrates. Design of the substrate was based on a dual-anchor model for specific binding that consists of displaying a functional group at the head (epoxide trigger) and the tail (amide functionality) of the otherwise hydrophobic poly-ene chain. The assay involved solubilization of the substrates with 0.2% surfactant. No ring formation was detected in the absence of antibody catalyst. The uncatalyzed epoxide hydrolysis was slow and did not deprive the antibody of substrate. Observations in the field of enzymic poly-ene cyclizations suggest that subtle changes in the substrate structure may well lead to multi-ring formation under the influence of the current catalyst.

Introduction

Poly-ene cyclizations are a fascinating class of biosynthetic unimolecular rearrangement reactions.¹ A large number of cyclase enzymes accept their respective substrate out of a pool of five natural candidates² to generate the astonishing diversity observed in the natural product class of the terpenes. A subclass among those enzymes transforms the triterpene squalene or its 2,3-epoxy derivative into pentacyclic (bacteria and protozoae) or, in the case of eukaryotes, either tetracyclic (via chair–boat–chair folding of oxidosqualene) or tetra- or pentacyclic products (via chair–chair–chair folding), respectively. Bacterial cyclases are considered primitive due to their lack of complete substrate and/or product specificity and the simple, thermodynamically favored cyclization mechanism involved; in contrast, the eucaryotic lanosterol synthase (OSC) has apparently reached maximum possible fidelity for the disfavored processes it carries out.^{3,4}

Cationic cyclizations are among the most demanding reactions that have been catalyzed by antibodies.⁵ These reactions have been studied mechanistically and recently the crystal structure of an antibody, which catalyzes a tandem cationic cyclization,⁶ has been elucidated.⁷ The outgrowth of this work opened up the possibility of catalytic formation of steroidal carbon

frameworks. However, biomimetic mono- or sesquiterpenoid-like substrates containing nonnatural leaving groups were used in these preceding investigations. Consequently, two remaining questions are whether antibodies are capable of cyclizing triterpene substrates and whether they can trigger cyclization starting from the natural leaving group, i.e., an epoxide oxygen.

Enzyme or catalytic-antibody poly-ene cyclizations can be divided into three stages: initiation, propagation, and termination. Crystallographic data from an antibody-catalyzed tandem cyclization have provided evidence that during propagation a strategy similar to nature's⁸ was adopted within the combining site. This antibody mainly utilized aromatic amino acid residues for the stabilization of high-energy cationic intermediates.⁹ During such an electrophilic addition event, precise orientation of a π -quadrupole moment and close proximity of the neighboring double bond toward their respective carbocation leads to an efficient decrease in activation energy that culminates in barrierless collapse.¹⁰ The initiation event as observed with oxidosqualene or squalene is believed to be triggered by an acidic catalytic motif (his-asp for squalene–hopene cyclase, SHC) which is buried at the bottom of the active cavity. *N*-oxides can strongly bind to this motif as has been demon-

(1) Sacchetti, J. C.; Poulter, C. D. *Science* **1997**, *277*, 1788–1789.
 (2) Geranyl-, farnesyl-, and geranylgeranyl pyrophosphate, squalene, and 2, 3-(*S*)-oxidosqualene.
 (3) (a) Abe, I.; Rohmer, M.; Prestwich, G. D. *Chem. Rev.* **1993**, *93*, 2189–2206. (b) Ourisson, G.; Rohmer, M.; Poralla, K. *Ann. Rev. Microbiol.* **1987**, *41*, 301–333.
 (4) For current developments in nonenzymic poly-ene cyclizations, see: (a) Sen, S. E.; Zhang, Y. z.; Smith, S. M. *J. Org. Chem.* **1998**, *63*, 4459–4465. (b) Xing, X.; Demuth, M. *Synlett* **1999**, *SI*, 987–989.
 (5) (a) Li T.; Janda K. D.; Ashley J. A.; Lerner R. A. *Science* **1994**, *264*, 1289–1293. (b) Hasserodt, J.; Janda, K. D.; Lerner, R. A. *J. Am. Chem. Soc.* **1996**, *118*, 11654–11655. (c) Li, T.; Janda, K. D.; Lerner, R. A. *Nature* **1996**, *379*, 326–327. (d) Li, T.; Lerner, R. A.; Janda, K. D. *Acc. Chem. Res.* **1997**, *30*, 115–121.

(6) (a) Hasserodt, J.; Janda, K. D.; Lerner, R. A. *J. Am. Chem. Soc.* **1997**, *119*, 5993–5998. (b) Hasserodt, J.; Janda, K. D. *Tetrahedron* **1997**, *53*, 11237–11256.
 (7) Paschall, C.; Hasserodt, J.; Jones, T.; Lerner, R. A.; Janda, K. D.; Christianson, D. W. *Angew. Chem., Int. Ed. Engl.* **1999**, *38*, 1743–1747.
 (8) (a) Wendt, K. U.; Poralla, K.; Schulz, G. E. *Science* **1997**, *277*, 1811–1815. (b) Wendt, K. U.; Lenhardt, A.; Schulz, G. E. *J. Mol. Biol.* **1999**, *286*, 175–187. (c) Starks, C. M.; Back, K.; Chappell, J.; Noel, J. P. *Science* **1997**, *277*, 1815–1820. (d) Lesburg, C. A.; Zhai, G.; Cane, D. E.; Christianson, D. W. *Science* **1997**, *277*, 1820–1824.
 (9) (a) Dougherty, D. *Science* **1996**, *275*, 1800–1804. (b) Lesburg, C. A.; Caruthers, J. M.; Paschall, C. M.; Christianson, D. W. *Curr. Opin. Struct. Biol.* **1998**, *8*, 695–703.
 (10) Jensen, C.; Jorgensen, W. L. *J. Am. Chem. Soc.* **1997**, *119*, 10846–10854.

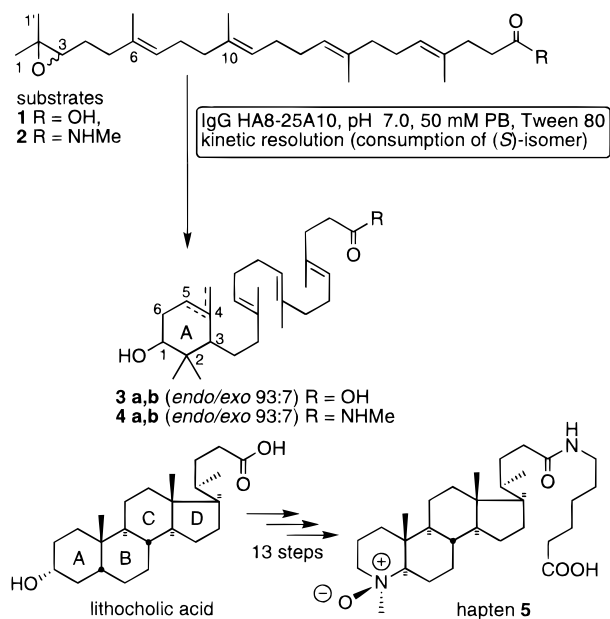


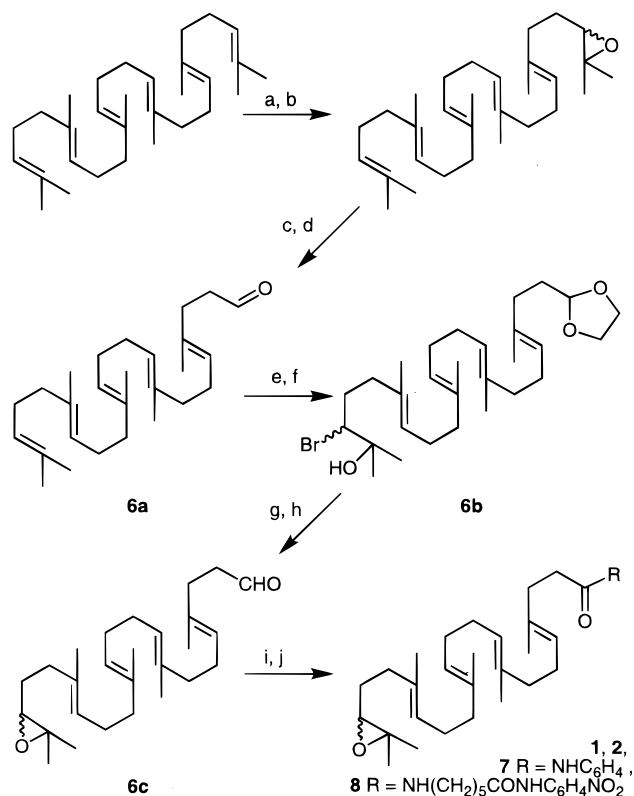
Figure 1. Antibody HA8-25A10 was induced by lithocholic acid-derived hapten **5** and stereoselectively catalyzed monocyclization of oxidosqualene derivatives **1** and **2** at neutral pH in an aqueous environment.

strated with various potent oxidosqualene cyclase inhibitors¹¹ and ultimately seen through a crystal structure.^{8a}

These combined observations coupled with results from antibody-catalyzed intramolecular hydroxyl attack on epoxides¹² led to the design and synthesis of optically pure hapten **5**, which is composed of a 4-aza-steroid skeleton derived from lithocholic acid (Figure 1).¹³ Lithocholic acid was chosen as a convenient starting material because it displays complete trans fusion between its rings B, C, and D. The configuration in its derivative **5** mimics a chair–chair–chair folding of the poly-ene substrate and thus represents a simpler cyclization mechanism compared to the one that OSC controls. Hapten **5** was linked through its “tail” (representing the latter part of the cyclization cascade) to keyhole limpet hemocyanin (KLH) so that the *N*-oxide moiety representing the initiation site would be most deeply buried in the antibody combining site.¹⁴ The complete antigen was then used to obtain a set of 25 monoclonal antibodies by standard hybridoma protocol.

Results and Discussion

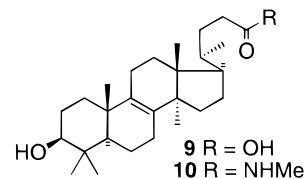
Initial testing for catalysis was carried out with two oxidosqualene derivatives, **1** and **2**, bearing two functional groups at their head and tail. This dual-anchor design, which is also displayed in hapten **5**, is expected to significantly increase substrate specificity while hydrophobic interactions should be the main contributor to binding energy.¹⁵ The synthesis of **1** and **2** was accomplished as shown in Figure 2. Compound **6a** was obtained via the Curphey/van Tamelen procedure.^{16a} Protection as a dioxolane, another bromohydrine formation to form **6b**, deprotection, and hydrogen bromide elimination to **6c**^{16b} were carried out by a sequence similar to that published



Conditions: a. NBS, THF/H₂O; b. K₂CO₃, MeOH; c. 3% HClO₄, DME, 35.5% over 3 steps; d. NaIO₄, THF, 77%; e. ethylene glycol, TsOH, PhMe, 97%; f. NBS, THF/H₂O, 30%; g. DBU, 99%; h. TsOH, acetone; i. AgNO₃, NaOH, THF, 57%; j. RNH₂, HATU, DMF, 81–23 %

Figure 2. Synthesis of oxidosqualene-derived substrates.

by Ceruti et al.^{16c} Subsequently, **6c** was transformed into substrate **1** with silver oxide. The various amide derivatives of **1** have been prepared by standard coupling procedures. With the present substrate design, the risk of product inhibition is likely to be low since formation of ring A of the steroid nucleus bearing a 3-hydroxyl group will diminish resemblance to the 4-aminoxide hapten design. The assay conditions for initial screening included solubilization of the hydrophobic substrates with a surfactant and running the reactions in phosphate buffer at neutral pH. The reactions were monitored simultaneously by thin-layer chromatography (TLC) (staining with anisaldehyde) and HPLC (210 nm). This dual assay system was necessary since simple UV monitoring by HPLC only showed products still containing two or three double bonds due to a low extinction coefficient. For example, a tetracyclized product like lanosterol derivative **9** or **10** could easily be TLC-detected in low concentrations through staining while remaining invisible in HPLC analyses coupled with UV detection.¹⁷



Three antibodies (15D6, 20C7, and 25A10), all obtained from immunization with hapten **5**, were selected for their ability to

(11) Cerutti, M.; Delprino, L.; Cattel, L.; Bouvier-Nave, P.; Duriatti, A.; Schuber, F.; Benveniste, P. *J. Chem. Soc., Chem. Commun.* **1985**, 1054–1055.

(12) Janda, K. D.; Shevlin, C. G.; Lerner, R. A. *Science* **1993**, 259, 490–493.

(13) Hasserodt, J.; Janda, K. D.; Lerner, R. A. *Bioorg. Med. Chem.* **in press**.

(14) Please note the reversal of substrate orientation when comparing this strategy (and the strategy by SHC) with an earlier concept. See ref 3b.

(15) Mader, M. M.; Bartlett, P. A. *Chem. Rev.* **1997**, 97, 1281–1301.

(16) (a) van Tamelen, E. E.; Curphey, T. J. *Tetrahedron Lett.* **1962**, 121–124. (b) Xiao, Y.; Prestwich, G. D. *J. Labelled Compd. Radiopharm.* **1991**, 29, 883–890. (c) Ceruti, M.; Rocco, F.; Viola, F.; Balliano, G.; Milla, P.; Arpico, S.; Cattel, L. *J. Med. Chem.* **1998**, 41, 540–554.

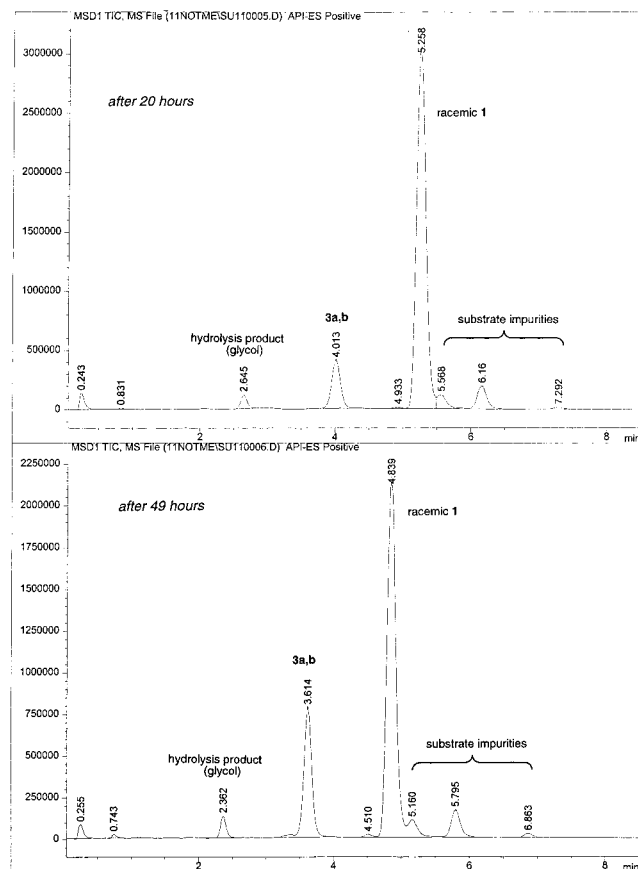


Figure 3. LC-MS chromatograms after 20 and 49 h of incubation. Conditions: IgG HA8-25A10 (24.6 μ M), substrate **1** (400 μ M), room temperature, 0.2% TWEEN 80, 50 mM PB, pH 7.0.

catalyze the initiation event. Comparatively large reactions (40 mL total volume, 17 μ M IgG, 9 mg substrate) yielded enough product (2.3 mg for **3a,b**) to allow characterization by NMR and LC-MS. High performance liquid chromatography (HPLC) coupled with an electrospray mass spectrometer (ESI-MS) is an ideal analytical system to monitor the antibody-catalyzed reaction. Since an isomerization reaction is analyzed, m/z values for substrates and products are the same, or, in the case of quenching of the terminal carbocations, increase by 18. The most prominent ions of interest were observed by Selected Ion Monitoring (SIM), which greatly enhances the sensitivity of the mass spectrometer for the detection of possible minor products. Figure 3 shows two chromatograms that provide a window into the 25A10-catalyzed transformation of **1** at different time intervals. Comparison of the retention time of **3a,b** with that of substrate and background product (glycol) revealed that the products have resulted from elimination as a termination pathway. Antibody 25A10 appears to effectively exclude water from the corresponding microenvironment in the active site as programmed by the hapten. Despite the strictly neutral conditions, substrate depletion due to hydrolysis to the corresponding glycol is clearly observed but negligible.

No ring formation was detected in the absence of antibody. This contrasts results of BF_3 -¹⁸ and CCl_3COOH -catalyzed¹⁹ transformations of a model compound (2,3-oxido-2,6-dimethylhept-6-ene) in organic solvents such as benzene, diethyl ether,

or chloroform. There, cyclization is observed, presumably via concerted oxirane cleavage. Under the aqueous conditions maintained in the antibody-catalyzed process, the presence of an abundant nucleophile evidently favors a reaction path involving water attack on the oxirane over anchimeric assistance by the neighboring double bond (despite the fact that cyclization would involve a thermodynamically favorable chair conformation). Also, the model reactions yielded complex mixtures of products in addition to the desired cyclized product, ranging from acyclic ketones to fluorohydrins.

Cyclohexenols **3a** and **4a** bearing an endocyclic 4,5-double bond were the principal products (93%) formed by all three catalysts from substrates **1** and **2**, respectively (Figure 1).²⁰ This ring system represents ring A of the lanosterol skeleton. Regioisomers **3b** and **4b** carrying an exocyclic double bond at C4 were found as minor products (7%) (in Figure 3, the traces for **3a** and **3b** are superimposed due to limitations of the column used).^{21,22} Interestingly, compounds **3b** and **4b** feature the same ring system as Achilleol A, biosynthesized by the plant *Achillea odorata* (Figure 6, A).²³

Any enantioselectivity by HA8-25A10 could not be determined by chiral HPLC. The optical antipodes of **3a** were not separated likely due to the incompatibility of the hydrophobic analytes with the relatively hydrophilic commercial chiral phases (e.g. amylose-based Chiralpak AD). Chiral GC on a β -cyclodextrin column also failed because of the low volatility of the methylated derivatives of **1** and **3**. Thus, **3a,b** was transformed into its methyl ester with diazomethane and then into the (*S*)- α -methoxy- α -trifluoromethyl- α -phenylacetic acid (MTPA) ester.²⁴ Proton NMR revealed only the presence of one major enantiomer as judged by the *dd* signals for H1 (93:7 for esters of **3a,b**). This result was supported by fluorine NMR that showed only one major signal and three insignificant ones.²⁵ However, an unambiguous determination of the enantiomeric excess was difficult due to the presence of **3b** (the signals of which cannot be distinguished reliably from those of **3a**). Hence, signals of the MTPA ester of **3b** could be mistaken for a minor amount of the MTPA diastereomer derived from the minor enantiomer of **3a**.

To garner information about possible enantiospecific substrate consumption, two consecutive reactions were allowed to proceed to approximately 15% and 50% conversion of racemic **1**, respectively (Figure 4). The remainder of **1** was recovered, methylated as above, and hydrolyzed to the glycol by 3% perchloric acid. The obtained glycol was then transformed selectively into the (*R*)-MTPA ester via the secondary hydroxyl group. Singlets *a* (1.181 ppm) and *b* (1.140 ppm) correspond to the diastereotopic methyl groups and signal *c* (5.105 ppm) to the chiral center of a single diastereomer. Multiplets *d+d'* (4.995 ppm) are the superimposed signals of both diastereomers corresponding to the neighboring olefinic position (determined

(20) The proton NMR spectrum displayed signals at 0.84 (s, 3H, C2-methyl), 0.97 (s, 3H, C2-methyl), and 3.47 ppm (dd, 1H, CHOH) consistent with the spectrum of Lanosterol-derived acid **9** and amide **10**. It also showed a signal at 5.16 ppm (m, 3H) for the three unchanged isoprenoidal double bonds and at 5.25 ppm (m, 1H) for the endocyclic double bond. The latter chemical shift is in accord with spectra from products with similar double bond substitution patterns in the literature.⁶

(21) Two characteristic proton NMR shifts for **3b** were detected at 4.60 (1H) and 4.90 (1H) ppm, which is in accord with literature data.^{6,23,28}

(22) The presence of a third, minor isomer with a double bond between C3 and C4 was not observed.

(28) Barrero, A. F.; Manzaneda, E. A.; Manzaneda, R. A. *Tetrahedron* **1990**, *46*, 8161–8168.

(29) (a) Dale, J. A.; Mosher, H. S. *J. Am. Chem. Soc.* **1973**, *95*, 512–519. (b) Ohtani, I.; Kusumi, T.; Kashman, Y.; Kakisawa, H. *J. Am. Chem. Soc.* **1991**, *113*, 4092–4096.

(30) See Supporting Information.

(17) See Supporting Information for synthesis scheme and NMR characterization.

(18) Goldsmith, D. J. *J. Am. Chem. Soc.* **1962**, *84*, 3913–3918.

(19) Corey, E. J.; Cheng, H.; Baker, C. H.; Matsuda, S. P. T.; Li, D.; Song, X. *J. Am. Chem. Soc.* **1997**, *119*, 1277–1288.

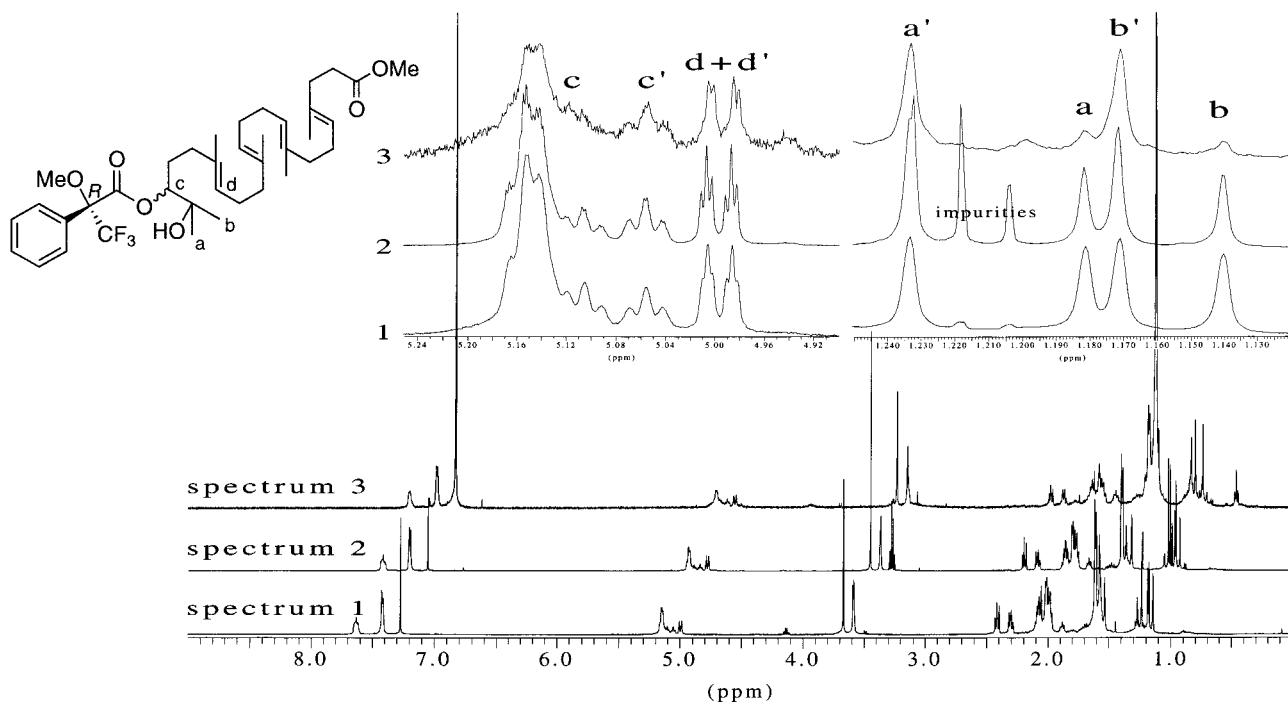


Figure 4. Determination of substrate enantiospecificity. Analysis was performed on remaining **1** after ca. 15% (spectrum 2: 9.0 mg) and ca. 50% (spectrum 3: 1.5 mg) consumption of the *racemic* substrate by the antibody. Spectrum 1: Authentic material. The remaining substrate was prepared for $^1\text{H-NMR}$ analysis by methylation (CH_2N_2), hydrolysis (HClO_4), and transformation into its (*R*)-MTPA ester. Enlarged regions are from 1.12–1.25 and 4.90–5.25 ppm.

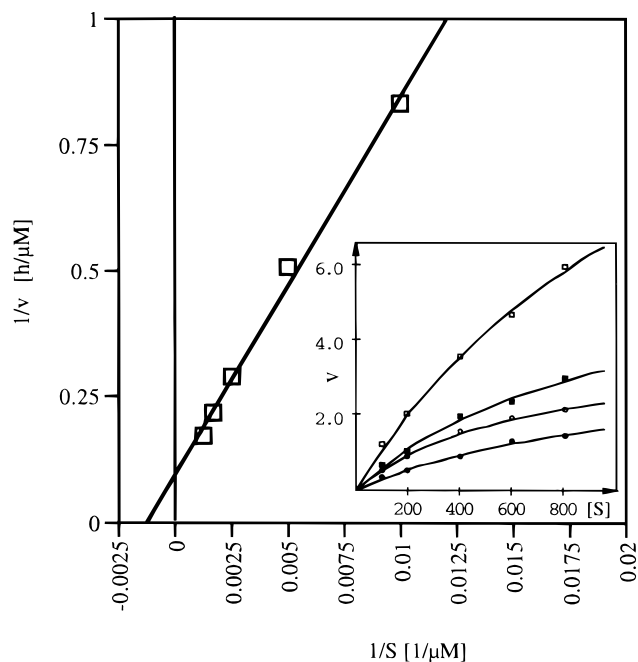


Figure 5. Lineweaver–Burk plot and Michaelis–Menten diagram (inset) of the reaction of IgG HA8-25A10 with substrate **1**. Conditions: $[\text{IgG}] = 5 \mu\text{M}$; 37°C ; 0.2% TWEEN 80; 50 mM phosphate buffer, pH 7.0; $[\text{I}] = 100, 200, 400, 600, 800 \mu\text{M}$. Complete saturation of the antibody was not possible due to solubility limits of **1**. Inset shows curves at hapten/inhibitor concentrations: $[\text{S}] = 0.0, 5.0, 7.5, 10.0 \mu\text{M}$.

by H,H-COSY). The decreasing intensities for one signal set unequivocally prove the preferred consumption of one enantiomer as seen with natural OSC.¹⁹ In contrast, certain SHCs have been observed to accept both enantiomers of oxidosqualene, their *nonnatural* substrate.³ Spectrum 3 allowed the estimation of an enantiomeric excess of 80% for the residual substrate after

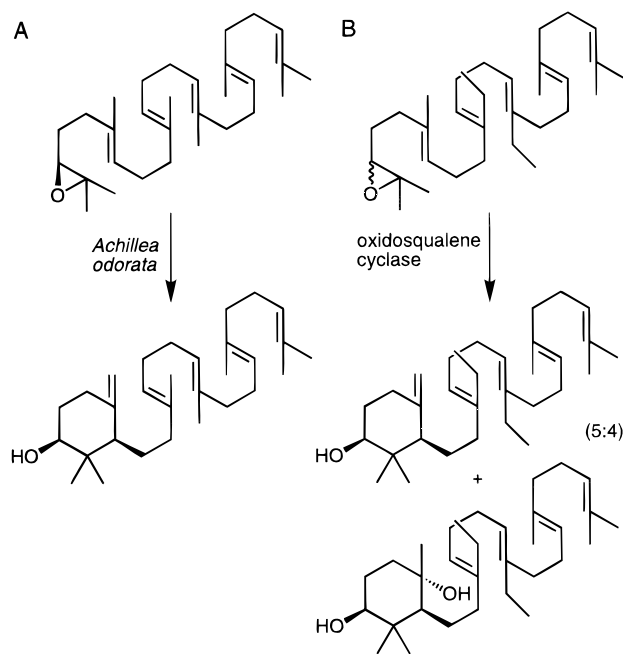


Figure 6. Monocyclization of oxidosqualene as part of a regular metabolic pathway (A) and as a result of an imperfect fit of a nonnatural substrate of oxidosqualene–lanosterol cyclase (B).

approximately 50% conversion. Further analysis of the (*R*)- and (*S*)-MTPA esters^{24b} derived from the minor enantiomer in the recovered substrate confirmed that (*S*)-**1**, in accordance with the absolute configuration of **5**, is the true substrate of HA8-25A10. If the transition state adopts a chair conformation, then it can be assumed that products **3a,b** show (1*S*,3*R*)-configuration as seen in the monocyclic products shown in Figure 6.

Kinetic analysis was carried out with the most proficient catalyst (HA8-25A10) and its best substrate (**1**). This catalyst

was initially tested for optimal performance with a variety of commercial surfactants.²⁵ HA8-25A10 showed maximum rates with TWEEN 80 and decanoyl-*N*-methylglucamide. The latter was dropped due to its low solubilizing power and high cost. All others impaired catalysis by various degrees with lauryl sulfobetaine as the only ionic detergent almost destroying catalytic activity. Cosolvents such as DMF and DMSO were ruled out for their significant reduction of catalytic rate as well as their strong absorption at 210 nm during HPLC assays where these solvents tended to bury the signals in question.

IgG HA8-25A10 showed saturation kinetics with $V_{\max} = 0.172 \mu\text{M min}^{-1}$, $k_{\text{cat}} = 0.017 \text{ min}^{-1}$, $K_M = 387 \mu\text{M}$ and a catalytic efficiency $k_{\text{cat}}/K_M = 44 \text{ M}^{-1} \text{ min}^{-1}$ (taking into account half the concentration of racemic substrate employed) (Figure 5). For comparison, only a few studies reporting kinetic parameters of triterpene cyclases are available to date. These tend to vary significantly because eukaryotic oxidosqualene cyclases are notoriously unstable during purification. While $k_{\text{cat}} = 3.38 \text{ min}^{-1}$ and $K_m = 18 \mu\text{M}$ were found for the cyclase of a yeast strain,¹⁹ another report quotes a $k_{\text{cat}} = 0.003 \text{ min}^{-1}$ and a similar $K_m = 15 \mu\text{M}$.²⁶ Also, a recent study characterized squalene-hopene cyclase (SHC) from the thermoacidophilic prokaryote *Alicyclobacillus acidocaldarius* that catalyzes a pentacyclization. The reaction proceeds by a simpler mechanism without any group migrations. This enzyme exhibits a k_{cat} of 300 min^{-1} and a K_m of $16.7 \mu\text{M}$ for squalene at its optimal temperature of $60 \text{ }^\circ\text{C}$.²⁷ Naturally, caution has to be taken when comparing the values exhibited by HA8-25A10 to the ones above, since a monocyclization is weighed against a multicyclization. At this point, the performance of the antibody and the triterpene cyclases may only be comparable in the substrate binding mode (including diffusion and the folding process) and possibly the mechanism of initiation. Future investigations will be used to unravel potentially important residues and the mechanism involved.

Hapten **5** competitively inhibited the catalytic antibody with a K_i of $9 \mu\text{M}$, demonstrating that the combining site carries the catalytic activity (Figure 5). Since the overall scaffolding in hapten **5** mimics propagation there is a certain risk of product inhibition in the case of multicyclization. The presence of lanosterol derivatives **9** and **10**, bearing the same tail functionalities as seen in substrates **1** and **2**, in the assay mixture did not result in any inhibition. Thus, it is reasonable to assume that **9** and **10** do not have a significant affinity toward HA8-25A10. However, only an experiment in the presence of a multicyclized product derived from lithocholic acid (but displaying the same substituents and configuration as ring A in lanosterol) will ultimately yield whether hapten **5** is sufficiently distinct from the desired products.

Two other derivatives of **2** were also tested with antibody HA8-25A10. While anilide **7** was not transformed, first experiments with nitroanilide **8**, featuring an aminohexanoate spacer, indicated it to be a substrate (Figure 2). This supports the conclusion that hapten **5** is buried entirely in the combining site, as was targeted by using a particularly long linker in this study. Additionally, the natural triterpene substrate 2,3-oxidosqualene in its racemic form was found not to be transformed by the antibody underlining the importance of the amide group in **1** and **2**. These results are in accord with the true aim of hapten design **5**, namely to induce a combining site that would specifically recognize the "head" and "tail" of the substrate thereby assisting the presumably less-specific hydrophobic

interactions and thus adding additional force to the folding of the poly-ene chain.

Conclusion

The stereoselective formation of monocyclic ring systems reflects the ability of the antibody catalysts to exert control over the initiation process. Thus, the step that needs particular enzymic assistance in biosynthetic oxidosqualene cyclization¹⁹ has been catalyzed by an antibody. However, propagation of cyclization for this particular class of substrates was not observed. Can multicyclization be accomplished by use of these catalytic antibodies? A recent finding showed that OSC produces a monocyclic product exclusively when charged with an 2,3-oxidosqualene analogue carrying two ethyl groups in place of the original methyls at C10 and C15 (Figure 6, B).²⁸ Evidently, minute changes in the substrate substitution pattern can dictate a productive versus a nonproductive conformation for the poly-ene chain in the active site. Consequently, the lack of constitutional congruency between the design of hapten **5** and substrates **1** and **2** may well be the cause for antibody HA8-25A10 to only produce monocyclic products. Theoretically, the best match to the hapten would include a hydrogen substituent at C10 in the substrate.²⁹ The single substitution at this location with a methyl group likely prevented productive binding for propagation. Fifty-three years ago, the equivalent for this conclusion was pointedly expressed by Linus Pauling for antibody-antigen recognition: "..., but that interference is caused [between a haptenic group and its antibody] by replacing a hydrogen atom (radius 1.2 \AA) by a methyl group."³⁰

Experimental Section

General. ¹H NMR (500 MHz) and ¹³C NMR (125 MHz) spectra were recorded on a Bruker AMX-500 instrument. Chemical shifts (δ) are given in ppm relative to CHCl_3 (7.27 ppm, ¹H; 77.00 ppm, ¹³C). High-resolution mass spectra (HRMS) were recorded at The Scripps Research Institute on a VG ZAB-ZSE mass spectrometer under fast atom bombardment (FAB) conditions. LC-MS analyses were performed on a Hewlett-Packard LC/MSD 1100 instrument.

Reactions were monitored by thin-layer chromatography (TLC), using 0.25 mm Merck Silicagel Glass Plates (60F-254), fractions being visualized by staining with *p*-anisaldehyde with subsequent heat application. Column chromatography was carried out with Mallinckrodt SilicAR 60 silicagel (40–63 μm). Reagent grade solvents for chromatography were obtained from Fisher Scientific. Reagents and anhydrous solvents were obtained from Aldrich Chemical Co. and used as is. Reported yields were determined after purification to homogeneous material.

22,23-Epoxy-1,1',2-trisnorsqualene-3-carboxylic Acid (1). A solution of AgNO_3 (20 mg in 0.38 mL H_2O) was added to a solution of NaOH (21 mg in 0.38 mL H_2O) with stirring. After 5 min, 22,23-epoxy-1,1',2-trisnorsqualene-3-aldehyde **6c**^{16b} (47 mg, 0.117 mmol) in 1.6 mL of THF was added to the suspension of black Ag_2O in one portion. After 40 min, 0.19 mL of a fresh suspension of Ag_2O was prepared according to the method above and added to the reaction mixture. Eighty minutes later, TLC indicated the reaction to be complete. Citric acid (5%) was added, and the mixture was extracted several times with ether. The combined organic phases were washed with brine and dried with MgSO_4 , and the residue was purified by silicagel chromatography (hexanes/ethyl acetate 8:1 \rightarrow 5:1, $R_f = 0.27$

(27) (a) Feil, C.; Poralla, K. *Eur. J. Biochem.* **1996**, *242*, 51–55. (b) Sato, T.; Kanai, Y.; Hoshino, T. *Biosci. Biotechnol. Biochem.* **1998**, *62*, 407–411.

(28) Hoshino, T.; Ishibashi, E.; Kaneko, K. *J. Chem. Soc., Chem. Commun.* **1995**, 2401–2402.

(29) This hypothesis will now be tested by synthesizing substrates displaying various methylation patterns to further probe antibody HA8-25A10.

(30) Pauling, L. *Chem. Eng. News* **1946**, *24*, 1375–1377.

(26) Moore, W. R.; Schatzmann, G. L. *J. Biol. Chem.* **1992**, *267*, 22003–22006.

[2:1], stains gray-blue). Yield: 28 mg (0.067 mmol, 57%). ¹H NMR (CDCl₃): 1.27 (3H, s), 1.31 (3H, s), 1.60 (3H, s), 1.61 (3H, s), 1.62 (6H, s), 1.63 (2H, m), 1.96–2.03 (8H, m), 2.06–2.11 (4H, m), 2.15 (2H, m), 2.31 (2H, m), 2.45 (2H, m), 2.74 (1H, t), 5.14–5.19 (4H, m). ¹³C NMR (CDCl₃): 16.0, 18.7, 24.8, 26.5, 26.6, 27.4, 28.2, 32.9, 34.3, 36.3, 39.5, 39.7, 58.6, 64.3, 124.3, 124.4, 124.9, 125.3, 132.9, 133.9, 134.8, 135.0, 178.8. HRMS (FAB, NBA/NaI) calcd for C₂₇H₄₄O₃ (M + Na⁺) 439.3188; found 439.3173.

Methylamide 2. A solution of **1** (134 mg, 322 μmol) in dry DMF (2.7 mL) was treated with methylamine hydrochloride (21.7 mg, 322 μmol), HATU (135 mg, 354 μmol), and diisopropylethylamine (DIEA) (167 mg, 1288 μmol, 4 equiv). After the mixture was stirred for 3 h at room temperature, 1 N citric acid was added, the mixture was extracted with ether, and the combined organic phases were extracted with water and brine and then dried over MgSO₄. Column chromatography (hexanes/ethyl acetate 6:1 → pure ethyl acetate, *R_f* = 0.20 [1:1], stains light brown) yielded a colorless oil (112 mg, 81%). ¹H NMR (CDCl₃): 1.27 (3H, s), 1.31 (3H, s), 1.61 (3H, s), 1.64 (3H, s), 1.60–1.70 (6H, m), 1.96–2.03 (8H, m), 2.06–2.11 (4H, m), 2.15 (2H, m), 2.28–2.32 (4H, m), 2.71 (1H, t), 2.80 (3H, d), 5.10–5.21 (4H, m), 5.54 (1H, s, broad). HRMS (FAB, NBA/NaI) calcd for C₂₈H₄₇NO₂ (M + H⁺) 430.3685; found 430.3704.

Anilide 7. Same procedure as for **2**, involving **1** (40 mg, 96 μmol), aniline (9 mg, 96 μmol), HATU (40 mg, 106 μmol), and DIEA (50 mg, 384 μmol) in dry DMF (800 μL). Column chromatography (hexanes/ethyl acetate 20:1 → 3:1, *R_f* = 0.42 [1:1], stains gray-brown) yielded a colorless oil (29 mg, 61%). ¹H NMR (CDCl₃): 1.39 (3H, s), 1.59 (3H, s), 1.60 (3H, s), 1.62 (3H, s), 1.64 (3H, m), 1.96–2.03 (8H, m), 2.06–2.11 (4H, m), 2.15 (2H, m), 2.39–2.46 (4H, m), 2.72 (1H, t), 5.13–5.16 (3H, m), 5.24 (1H, t), 7.09 (1H, t), 7.30 (2H, t), 7.50 (2H, d), 7.63 (1H, s, broad). HRMS (FAB, NBA/NaI) calcd for C₃₃H₄₉NO₂ (M + Na⁺) 514.3661; found 514.3673.

Nitroanilide 8. Same procedure as for **2**, involving **1** (147 mg, 353 μmol), 6-aminocaproic *p*-nitroanilide²⁵ (93 mg, 394 μmol), HATU (161 mg, 106 μmol), and DIEA (102 mg, 788 μmol) in dry DMF (3.2 mL). Column chromatography (hexanes/ethyl acetate 10:1 → pure ethyl acetate, *R_f* = 0.38 [ethyl acetate]) yielded a colorless oil (53 mg, 23%). ¹H NMR (CDCl₃): 1.26 (3H, s), 1.30 (3H, s), 1.38 (2H, m), 1.54 (2H, m), 1.59 (9H, m), 1.61 (3H, s), 1.62 (1H, m), 1.76 (2H, m), 1.94–1.20 (8H, m), 2.04–2.08 (5H, m), 2.15 (1H, m), 2.29 (4H, s), 2.42 (3H, t), 2.72 (1H, t), 3.25 (2H, q), 5.12–5.16 (4H, m), 5.94 (1H, t, broad), 7.80 (2H, d), 8.17 (2H, d), 9.07 (1H, s, broad). ¹³C NMR (CDCl₃): 16.0, 18.7, 24.6, 24.9, 26.6, 27.4, 28.2, 29.1, 35.4, 36.3, 37.0, 39.0, 39.5, 39.6, 58.5, 64.3, 119.0, 124.3, 124.4, 124.9, 125.5, 133.3, 133.9, 134.8, 135.0, 143.0, 144.6, 172.2, 173.4.

Tris-nor-lanosterol-24-carboxylic Acid (9).³¹ This already published compound has been synthesized from commercial lanosterol (TCIAmerica No. C0427) by a novel procedure outlined in the Supporting Information. ¹H NMR (CD₃OD): 0.73 (3H, s), 0.80 (3H, s), 0.90 (3H, s), 0.93 (3H, d), 0.97 (3H, s), 1.00 (3H, s), 2.23 (1H, m), 3.14 (1H, dd). The proton NMR spectrum is in accord with that in the literature.³¹ HRMS (FAB, NBA/NaI) calcd for C₂₇H₄₄O₃ (M + Na⁺) 439.3188; found 439.3177.

N-Methyl-tris-nor-lanosterol-24-carboxamide (10). This compound has been synthesized according to the procedure for methylamide **2**: 3-Acetyl-tris-nor-lanosterol-24-carboxylic acid²⁵ (77 mg, 168 μmol), methylamine hydrochloride (11.8 mg, 174 μmol), HATU (73 mg, 192 μmol), DIEA (90.5 mg, 698 μmol, 4 equiv), and 1.5 mL of anhydrous DMF. Column chromatography (hexanes/ethyl acetate 5:1 → ethyl acetate, *R_f* = 0.40 [ethyl acetate], stains gray-blue) yielded 68 mg (86%) of product. This material was then deacylated by refluxing it for 10 min in 9 mL of MeOH (containing 230 mg NaOH). *R_f*(**10**) = 0.37, with tailing [ethyl acetate], stains gray-blue also. ¹H NMR (CDCl₃): 2.24 (1H, m), 2.80 (3H, d), 3.23 (1H, dd), 5.51 (1H, s, broad). LRMS (FAB, NBA/NaI) calcd for C₂₈H₄₇NO₂ (M + Na⁺) 453; found 453.

(31) Bernassau, J. M.; Fetzion, M. *Synthesis* **1975**, 795–796 and references therein.

Hybridoma Production. See ref 5b.

Screening of Anti-5 Antibodies. All 25 clones were first tested in reactions with a total volume of 200 μL in microvials. These consisted of a 50 μL stock solution of substrate (800 μM in 50 mM phosphate buffer PB, pH 7.0, 0.2% Triton-X 100), varying amount of IgG stock solution depending on individual clone (in PB), and PB (remaining volume to complete total). Final concentrations: [IgG] = 16.5 μM; [S] = 200 μM. After incubation (48 h, 37 °C), all reactions were directly analyzed by HPLC (Phenomenex Luna 3μ C8(2) 150 × 4.6 mm; isocratic at CH₃CN/H₂O 85/15 (0.1% TFA); 210 nm). IgGs that showed substrate depletion were reintroduced into 2 mL reactions with the same concentrations as above. The samples obtained by extraction with 2 mL of CHCl₃, centrifugation at 3000 rpm for 10 min to separate phases, and evaporation of the solvent from the organic phases were spotted on TLC plates and analyzed in ethyl acetate/ethanol 9:1. For substrate **1**, anisaldehyde stained background product (glycol) brown, products blue, and substrate brown again (in the order of increasing *R_f* values).

LC-MS. Reactions of HA8-25A10 with substrate **1** were analyzed with Phenomenex Luna 3μ C18(2) 30 × 2.00 mm, 0.8 mL/min flow, 32 °C, gradient [“A” = H₂O, 0.05% TFA]/[“B” = CH₃CN, 0.05% TFA] 50% B–1 min–60% B–6 min–80% B, then 100% B. MS detector was set to 399.5 (M – H₂O + H⁺), 417.5 (M + H⁺) and 435.5 (M + H₂O + H⁺) (SIM).

Scale-Up for Identification of Product 3a,b and Its Transformation into the MTPA Ester. Reaction setup: 40 mL total volume; 10 mL HA8-25A10 (10.3 mg/mL) in PB (50 mM, pH 7.0); 0.858 mL substrate **1** (25 mM, 8.92 mg) in PB (15% Triton-X 100); 29.1 mL PB (50 mM, pH 7.0); 37 °C. After 4 days, no further progress of the reaction could be detected. The slightly turbid solution was then extracted with CHCl₃, phase separation was achieved by filtration through Celite, the organic phase was dried (MgSO₄), treated with an ether solution of CH₂N₂ for 20 min, and evaporated. The residue was passed through a short silicagel column with the aid of ethyl acetate to remove the detergent. A second column then provided methylated products **3a,b** (hexanes/ethyl acetate 10:1 → 3:1, *R_f* = 0.33 [3:1], stains blue). Yield: 2.3 mg (5.35 μmol, 50%, calculated for consumption of (S)-**1**) and ca. 5 mg of methylated **1** (82% recovered material, remainder consisted of the glycol that is formed in the background reaction). ¹H NMR (**3a,b**, CDCl₃): 0.84 (3H, s), 0.98 (3H, s), 1.57–1.73 (12H, m), 1.97–2.08 (14H, m), 2.12–2.24 (1H, m), 2.30 (2H, m), 2.40 (2H, m), 3.47 (1H, dd), 3.67 (3H, s), 4.61 (1H, m, **3b**), 4.88 (1H, m, **3b**), 5.15 (3H, m), 5.25 (1H, m). This material was subsequently transformed into its (S)-MTPA ester with (R)-(–)-α-methoxy-α-(trifluoromethyl)-phenyl acid chloride according to a literature procedure.^{24a} HRMS for the MTPA ester of **3a,b** (FAB, NBA/NaI) calcd for C₃₈H₅₃F₃O₅ (M + Na⁺) 669.3743, found 669.3773.

Acknowledgment. Financial support was provided by The Scripps Research Institute (J.H.), The National Institutes of Health (GM-43858), The Skaggs Institute for Chemical Biology (K.D.J.). Help with the hybridoma work by Ping Fan and Alisa Moore, as well as expert assistance with the LC-MS analyses by Geoffrey Barker and Dr. Gary Siudzak, is gratefully acknowledged.

Supporting Information Available: A listing of proton/carbon NMR spectra of **1** and **2** and their synthetic intermediates, of **7–10**, proton NMRs of antibody products **3a,b**, its (S)-MTPA ester, **4a,b**, determination of absolute configuration of true substrate (**1**), detergent evaluation, typical LC-MS and conventional HPLC chromatograms of the antibody-catalyzed reaction as well as product distribution (PDF). This material is available free of charge via the Internet at <http://pubs.acs.org>.